Journal of Petroleum Research and Studies

Open Access
No. 38, March 2023, pp. 56-73

P- ISSN: 2220-5381
E- ISSN: 2710-1096

DOI: http://doi.org/10.52716/jprs.v13i1.680

Intelligent Approach for Investigating Reservoir Heterogeneity Effect on Sonic Shear Wave

Jassim M. Al Said Naji[1*], Ghassan H. Abdul-Majeed[2], Ali K. Alhuraishawy[3]

[1,2]University of Technology, Baghdad, Iraq

[1]University of Baghdad, Baghdad, Iraq

[3]Ministry of Oil, Baghdad, Iraq

[1*]Corresponding Author E-mail: 150100@uotechnology.edu.iq.

[2]ghassan@uob.edu.iq.

[3]ali19_82@yahoo.com.

Received 24/7/2022, Accepted in revised form 10/8/2022, Published 15/3/2023

Abstract

Heterogeneity refers to a not uniform distribution of reservoir properties. To overcome the problem of heterogeneity, most reservoir studies split the reservoir into different zones. In general, this disparity affects all log tools. Sonic shear wave time (SSW) is a critical metric in geomechanical modeling that is strongly influenced by reservoir heterogeneity and the kind of porous fluid composition. To detect the effect of reservoir heterogeneity on SSW prediction, an artificial neural network (ANN) was applied as an intelligent technique. One Iraqi vertical well that penetrated the Asmari reservoir was selected for this study. It contains 2462 SSW measured points as well as the following seven log parameters: Gamma Ray, Caliper, Density, Neutron, Compressional sonic, and True resistivity log over measured depth. Based on formation assessment and available well data, the Asmari reservoir was classified into six zones (with different lithology and different fluid content): A, B1, B2, B3, B4, and C. To investigate the effect of lithology on SSW, two runs of ANN had been conducted in this study.

Initially, we developed a single ANN for all 2462 measured points, while in the second, six ANNs were built, one for each zone. The optimum structure for all the developed ANNs was obtained with one hidden layer of 12 neurons (7-12-1). The statistical parameters used for comparison are average percent error (APE), absolute average percent error (AAPE), standard deviation (SD), mean square error (MSE), and correlation coefficient (R2). It was observed that these parameters are approximately close to each other for the developed seven ANNs. The R2 values of the seven ANNs are 0.98 for all zones, and 0.99, 0.99, 0.99, 0.99, 0.99 and 0.96 for each zone respectively. The insignificant differences of results can be explained by the fact that the log readings (i.e. inputs variables) are already reflected the effect of lithology. Therefore, we

Open Access
No. 38, March 2023, pp. 56-73
P- ISSN: 2220-5381
E- ISSN: 2710-1096

recommended using the ANN based on 2462 for predicting SSW to any lithology zone. A mathematical model for representing the suggested ANN to simplify the calculation.

Keywords: Reservoir heterogeneity, Zonation, Sonic shear wave, Artificial neural network, Empirical correlations.

1. Introduction

Heterogeneity of oil and gas reservoirs is defined as special distribution of rocks properties in nonlinear and non-uniform way [1]. Many authors stated that heterogeneity is related to change of properties at any place in three dimensions of reservoir system [2, 3] while others add time as a four-dimension causing heterogeneity due to changing of properties with it [4] so any reservoir property i.e., porosity is changing with place from point to another, reservoir will be heterogeneous with respect to porosity and if it constant with location, it is called homogenous reservoir. A reservoir is known as isotropic to any property if this property doesn't change with direction while it is called anisotropic if a property changes with direction. A common example of reservoir isotropic and anisotropic is permeability changing with direction. Horizontal permeability is almost greater than vertical permeability due to the thin shale layers' effect on last. If permeability is the same in all direction so porous media will be isotropic and if not, it will be anisotropic [5]. Figure (1) is showing reservoir states of heterogeneity, homogeneity, isotropic and anisotropic [6]. All log measurements are highly sensitive to borehole and its environment according to effects of hole size and drilling fluids, radial changes in environment around wellbore due to mud invasion, and vertical heterogeneity caused by different layers thickness. In addition, log tools have limited range of investigation radius as in Figure (2), so they will give different responses in heterogeneous formations where their measurements are characterized by vertical resolution and radius of investigation [7].

Open Access
No. 38, March 2023, pp. 56-73
P- ISSN: 2220-5381
E- ISSN: 2710-1096

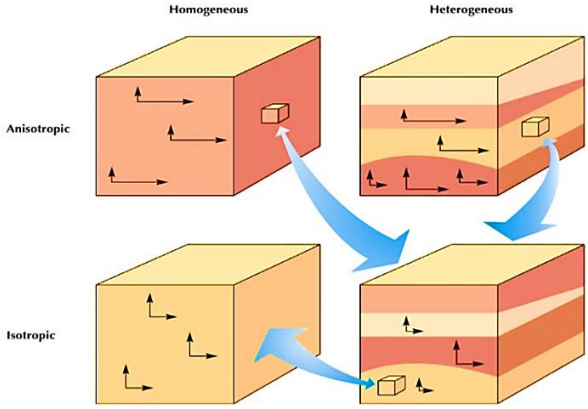

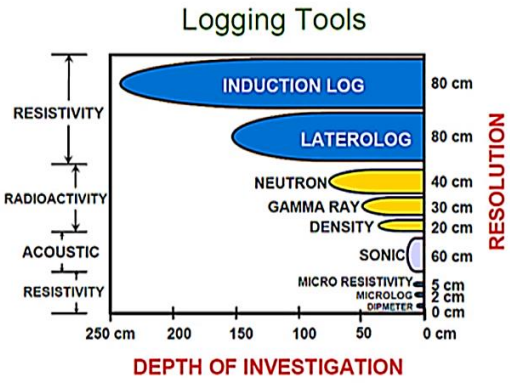

Fig. (1): Illustration of reservoir lithology state [6]. **Fig. (2): Radius of investigation of log tools [7]**

Compressional and shear sonic wave times (*CSW* and *SSW*) are important parameters in calculating elastic rocks properties that represent a key for geomechanics modeling to study wellbore instability and sand production prediction [8] as well as gas bearing zones identification and gas saturations estimation [9]. Four ways are existing for *SSW* determination, logging method and laboratory core measurements, and are predicted by theoretical and statistical approaches [10] but in some reservoir intervals *SSW* is not running due to high measurements cost [11]. Since the sixties of the last century, many empirical correlations were developed to determine SSW for different rock types formation [9, 12, 13, 14, 15, 16, 17, 18]. All developed empirical correlations are calculated shear sonic velocity (*SSV*) based on compressional sonic velocity (*CSV*) in velocity unit (km/sec) where:

$$SSV = \frac{1}{SSW} \tag{1}$$

$$CSV = \frac{1}{CSW} \tag{2}$$

Three Global empirical correlations from mentioned above are suitable for all reservoir types,

An empirical correlation introduced by Carroll for *SSV* predicting. He studied effects of rock types and hydrostatical loads on *SSV* estimating by trained 62 tested dry cores and measured logs data from different intervals from the volcanic region of Nevada. His correlation had the following formula [13]:

$$SSV = 0.75609.CSV^{0.81846} \tag{3}$$

An empirical correlation developed by Freund appropriate for all reservoir types to predict

Open Access
No. 38, March 2023, pp. 56-73
P- ISSN: 2220-5381
E- ISSN: 2710-1096

SSV by using tests of 57, 25 and 5 samples of sandstone, siltstones and claystone respectively for well penetrated Rotliegendes reservoir in Germany. The developed correlation is [16]:

$$SSV = 0.763.CSV - 0.603 \quad (4)$$

Another empirical correlation established by Brocher to estimate SSV based on different *CSV* and *SSV* with tested cores collected from different fields in California. Established correlation can be using for any reservoir [17]:

$$SSV = 0.7858 - 0.1244.CSV + 0.7949.CSV^2 - 0.21238.CSV^3 + 0.006.CSV^4 \quad (5)$$

A novel empirical correlation provided to quantify *SSW* in terms of *CSW* utilizing 1922 observed data from one Iraqi directional well. It is good for all reservoir types and is especially appropriate for reservoirs in southern Iraq, as seen below [19]:

$$SSW = -0.0143.CSW^2 + 3.1521.CSW - 29.73 \quad (6)$$

Different in properties of reservoir layers that have different fluid types distributed in pores is one of influencing parameters on *SSW* measurements and prediction where sonic waves velocity reduces if shale existing in reservoir layers and liquid wet porous [20]. To consider as much possible as large number of influencing parameters on *SSW* prediction, authors worked on using different approaches of artificial intelligent (*AI*) such as artificial neural network (*ANN*), fuzzy logic, and neuro-fuzzy system with participation more than datasets such as *CSW*, gamma ray (*GR*), caliper (*CAL*), deep resistivity log (*DRL*), density log (*DL*), neutron log (*NL*) and measured depth (*MD*) to represent different in rocks types, hole size effects, fluid types, porosity and lithology, and overburden pressure respectively [11, 21, 22, 23]. Applications of *ANN* in oil and gas industry begun since 1990 [23].

This paper aimed to investigate the effect of reservoir heterogeneity on *SSW* prediction by *ANN* using logs data of one Iraqi vertical X well.

1.1. Area of Study and Reservoir Lithology

Y- oil field exists in Missan governorate at south of Iraq. It is a way 175 km north of Basrah city and 50 km to north–east of Ammara city as shown in Figure (3). From the east, this field extend along the Iraq - Iran borders near Iraqi Buzrgan oil field. It has two domes with north-west, south-east anticline in north and south respectively. Field length is about 23 km and width is about 7 km. It is producing from two main formations Mishrif and Asmari. The first well drilled

Open Access
No. 38, March 2023, pp. 56-73
P- ISSN: 2220-5381
E- ISSN: 2710-1096

in this field at 1973 reached to depth 4683 m and was produced from both mentioned reservoirs. Asmari is an Iranian name but Iraqi reservoir studies are classified it into three reservoirs Jeribe Euphrates, Upper Kirkuk and Middle-Lower Kirkuk as described in stratigraphic column of Y field at Figure (4). Mostly this formation classified as a semi heterogenous because it consisted from many rock types as shale, carbonate and sandstone with a number of fractures. Previous studies classified Asmari reservoir into four zones A, B, C, and D but modern studies divided it into main three zones A, B and C where D merges with C entitled C according to submerging in water. A has three subzones A1, A2, and A3 while B has four subzones B1, B2, B3, and B4 according to fluid content kinds and rock typing as shown in Table (1) [24, 25].

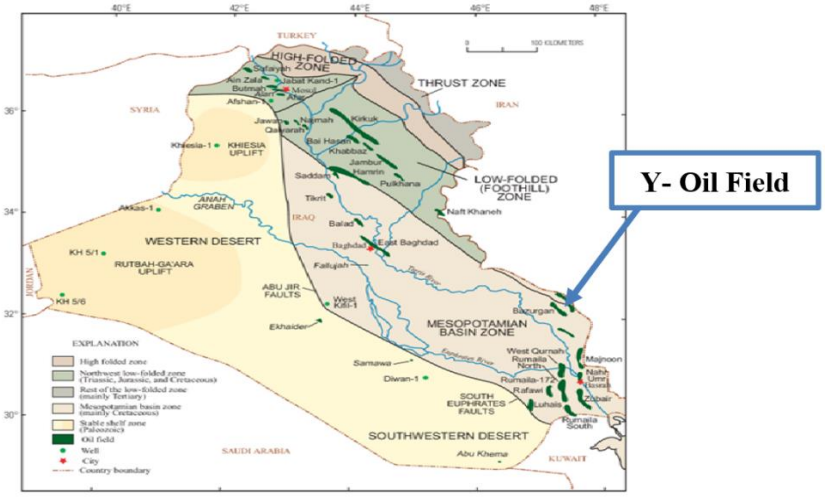

Fig. (3): Location of Iraqi Y oil field Iraq map [26].

Table (1) Summary of geological description of Asmari formation / Y oil field [25].

Formation	Average Thickness (m)	Zones	Subzones	Lithology
Jeribe Euphrates	40	A	A1, A2, and A3	**Little anhydrate and shale intercalated with dolomite**
Upper Kirkuk Formation	120	B	B1, B2, B3, and B4	**Shale intercalated with sandstone, limestone, and dolomite.**
Middle-Lower Kirkuk Formation	200	C	-	**Argillaceous limestone intercalated with sandstone, argillaceous siltstone and calcareous shale.**

Open Access
No. 38, March 2023, pp. 56-73

P- ISSN: 2220-5381
E- ISSN: 2710-1096

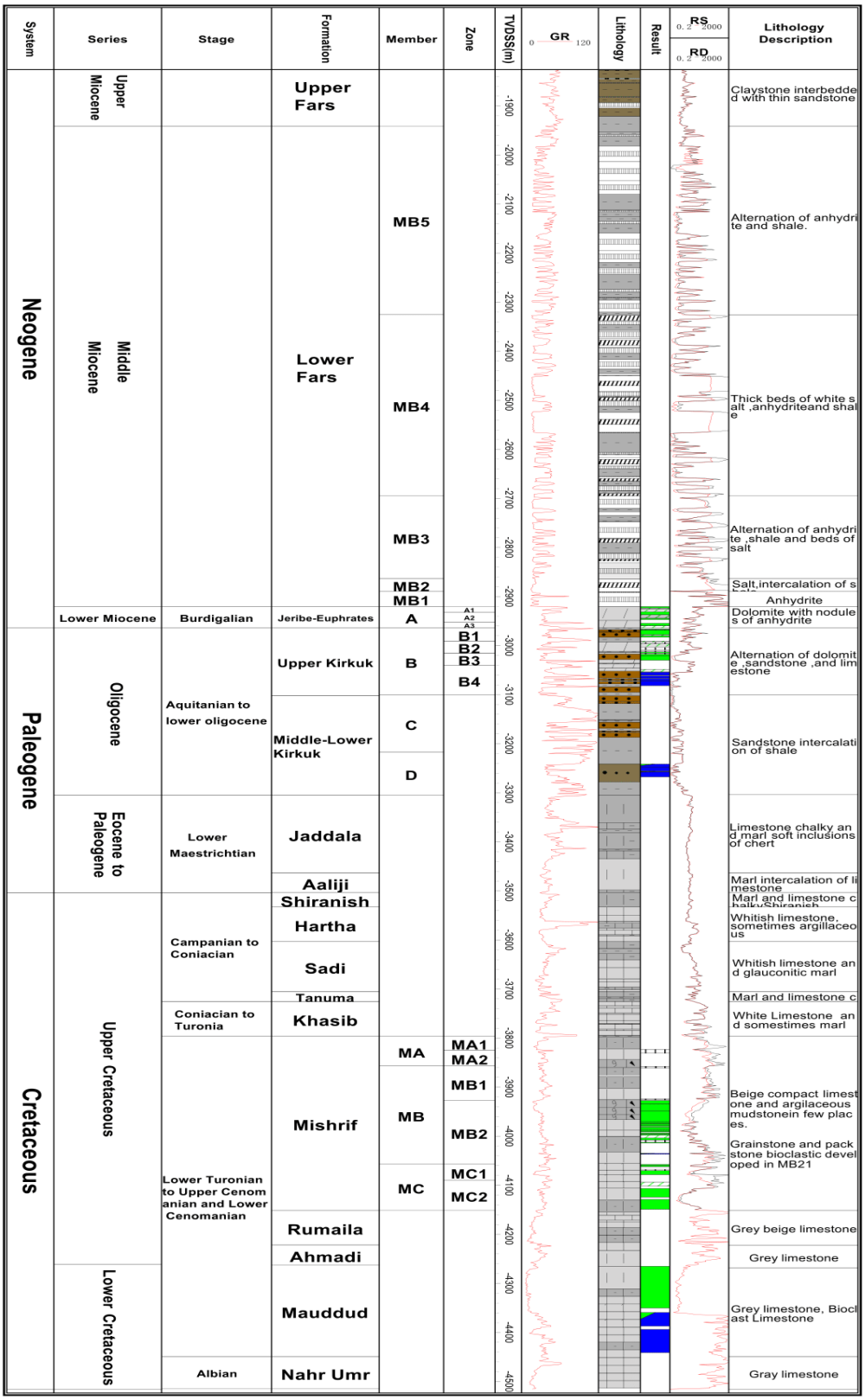

Fig. (4): Stratigraphic column of Y oil field [25].

Open Access
No. 38, March 2023, pp. 56-73
P- ISSN: 2220-5381
E- ISSN: 2710-1096

2. Materials and Methods

Reservoir heterogeneity is an uneven change in internal properties and its spatial distribution caused by effects of sedimentary environment, diagenesis, and tectonic processes during the formation process [27] where Table (1) showed that Asmari reservoir consisted from different lithologies, so, to overcome this challenge, formation is re-evaluated based on a number of wells data due to different in lithology and its fluid content. It is classified to six zones: A, B1, B2, B3, B4 and C.

In present study measured logs of one vertical X well penetrated Asmari six zones in Y oil field used as database for *SSW* prediction by *ANN*. The vertical well dataset comprised 2462 measured points related to all zones of *SSW* beside others logs of *GR*, *CSW*, *CAL*, *NL*, *DL*, *DRL* with *MD* as present in Figure (5).

Two runs of *ANN* were performed in this study to investigate the effect of lithology on *SSW*. In the first, we proposed *ANN* for all 2462 measured points, but in the second, we constructed six *ANNs*, one for each zone. Table (2) displays vertical well tops and bottoms at Asmari reservoir zones, together with the number of measured points for each zone.

Table (2) Utilized vertical well top, bottom and number of measured points at each zone.

Zone	Top	Bottom	No. of measured points
A	3003	3051	472
B1	3051	3088	370
B2	3088	3105	170
B3	3105	3123	180
B4	3123	3177	540
C	3177	3250	730

ANN had been utilized due to its ability to learn from examples, low cost, efficiency and ease of understanding where it is used in many studies to predict parameters that mostly cannot estimate by common ways [28]. For two runs, *ANNs* are designed using MATLAB R2012b in term of multiple layer perceptron (*MPL*) with one hidden layer. *MPL* is a commonly used of *ANN* types where data processing accomplishes in one direction without any loops [29]. It is consisting of three layers, an input layer for input parameters, an output layer for output results and a single or multi hidden layer as a connection between input and output layers. Each layer has number of neurons connected with others in sequent layer with parameter called weight (*Wi*) while some of freedom degree to neurons is added by a parameter called bais (*bi*) [30].

Open Access
No. 38, March 2023, pp. 56-73

P- ISSN: 2220-5381
E- ISSN: 2710-1096

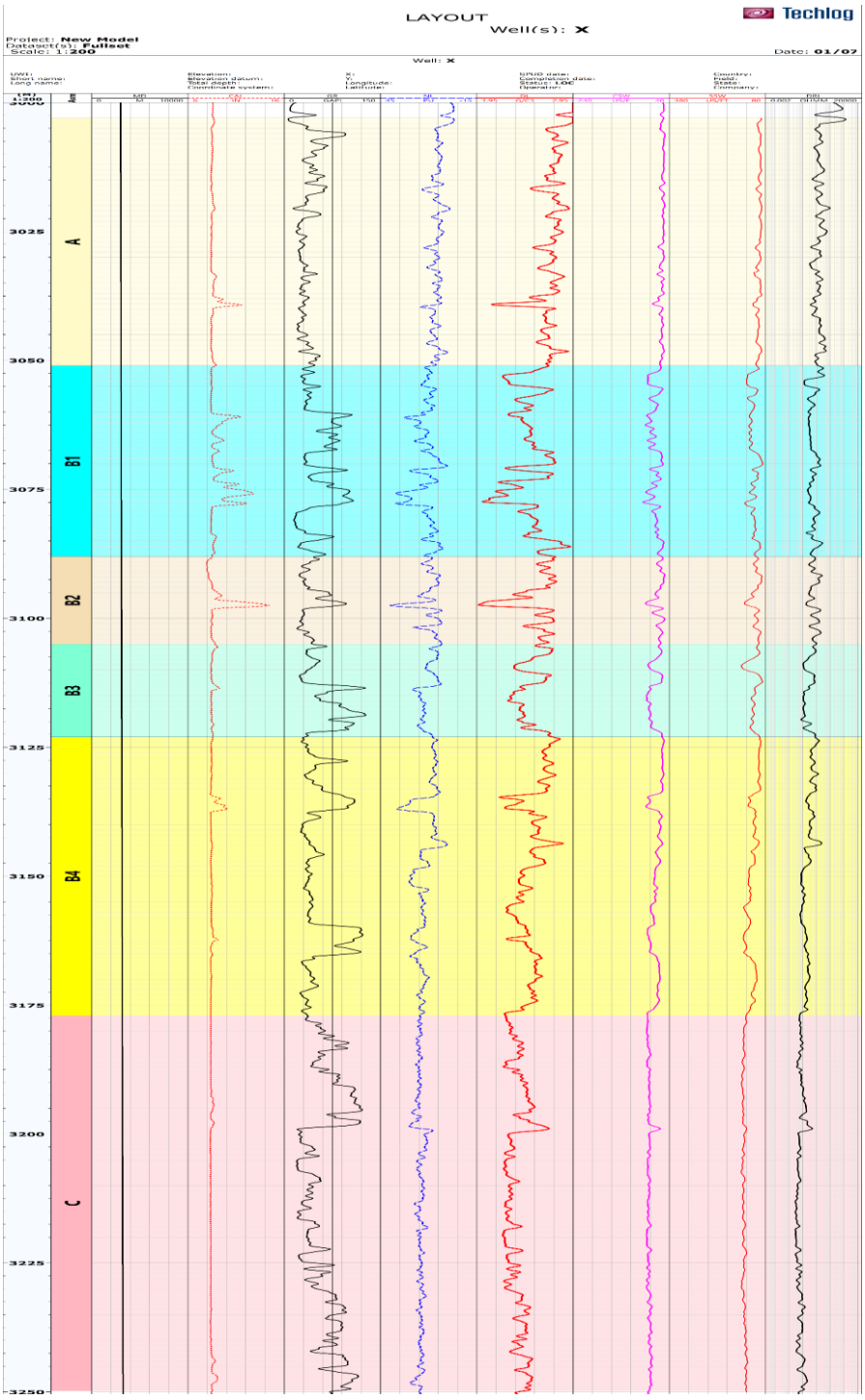

Fig. (5): Vertical X well log tracks.

ANN is processed by three subsequent processes training, validation and testing and mostly, datasets classified according to these processes as 70%, 15% and 15% respectively. The following equation is representing of effecting of hidden or output neurons in term of

Open Access
No. 38, March 2023, pp. 56-73
P- ISSN: 2220-5381
E- ISSN: 2710-1096

participating and enhancing of each inputted neuron of previous layers as cross summation [31]:

$$S_j = \sum_{i=1}^{n} X_i \, W1_{ji} + \, b1_j \tag{7}$$

Hyperbolic tangent function is adopted as an activation function for the hidden layer while the liner function is used for output layer activation as shown in following **Eq.8** and **Eq.9** respectively where output resulted in term (-1, 1) [32]:

$$f(S_j) = \frac{2}{1+e^{-2\,S_j}} - 1 \tag{8}$$

$$T_P = \sum_{j=1}^{k} W2_j \; f(S_j) + b2_j \tag{9}$$

Where $W1_{ji}$ is a connection weight between the input vector X_i and hidden layer neurons j, S is a summation of weights between biases, $b1j$ and inputs, n represent the neurons number of input layer. T_p is the predicted (*SSW*) result value, $W2_j$ is the output hidden layer weight, $b2_j$ is the bias of output layer, while k is the hidden layer neurons.

Adopting seven log parameters of *GR*, *CSW*, *CAL*, *NL*, *DL*, *DRL* with *MD* for *SSW* prediction was based on the impact of these paraments on *SSW* proven by different literatures [19, 24, 33, 34, 35, 36] where *MD*, *DRL* and *DL* had a negative impact on *SSW*, *CSW* and *NL* had a positive effect while *GR* and *CAL* had a dual impacting on it.

2.1. Single ANN for All Reservoir Zones

One *ANN* with single hidden layer is constructed for *SSW* prediction by using all 2462 measured points. The seven mentioned log parameters used as neurons of the input layer of *ANN* while *SSW* as the output layer neuron. Table (3) shows a summary of utilized datasets.

Table (3) Summary of all zones data.

Parameter	Minimum	Maximum	Mean
SSW (us/ft)	89	156.2	123.1
MD (m)	3003.9	3250	3126.95
CSW (us/ft)	47.4	89.448	68.77
GR (GAPI)	14.285	126.914	52.34
CAL (in)	7.948	14.436	8.58
NL (%)	0.331	39.033	16.19
DRL (ohm.m)	0.285	94.216	6.35
DL (gm/cc)	1.969	2.947	2.51

Open Access
No. 38, March 2023, pp. 56-73
P- ISSN: 2220-5381
E- ISSN: 2710-1096

2.2. ANN for Each Zone

Single hidden layer *ANN* is made for each zone to reflect the effect of lithology and fluid contents, using the datasets listed in Table (2) (column 4). Six *ANNs* were constructed by using datasets that summarized in Tables (4) and (5).

Table (4) Dataset summary of A, B1 and B2 zones

Parameter	A zone			B1 zone			B2 zone		
	Min	Max	Mean	Min	Max	Mean	Min	Max	Mean
SSW (us/ft)	91.86	119.61	100.5	89	144.2	117.97	91.48	145.8	109.44
MD (m)	3003.9	3051	3027.45	3051.1	3088	3069.55	3088.1	3105	3096.55
CSW (us/ft)	47.4	71	54.22	51	89.448	69.32	50.33	85	60.52
GR (GAPI)	14.285	95.736	37.02	14.957	107.65	52.19	20.12	96.56	41.001
CAL (in)	8.394	11.553	8.56	8.357	12.768	9.01	7.948	14.44	8.82
NL (%)	0.33	20.35	9.89	3.589	35.624	16.14	6.704	39.03	13.68
DRL (ohm.m)	3.17	94.22	18.15	1.264	37.148	7.25	1.739	24.99	8.38
DL (gm/cc)	2.106	2.947	2.72	2.008	2.923	2.49	1.969	2.774	2.589

Table (5) Dataset summary of B3, B4 and C zones.

Parameter	B3 zone			B4 Zone			C Zone		
	Min	Max	Mean	Min	Max	Mean	Min	Max	Mean
SSW (us/ft)	89	155.8	116.65	95.09	149.8	120.05	135.8	156.2	147.33
MD (m)	3105.1	3123	3114.05	3123.1	3177	3150.05	3177.1	3250	3213.55
CSW (us/ft)	53.8	86.6	72.025	50.57	86.6	65.343	63.16	86.61	81.56
GR (GAPI)	23.9	126.9	64.56	24.89	121.9	51.48	19.27	121.74	62.59
CAL (in)	8.39	9.27	8.53	8.336	10.1	8.48	8.314	9.068	8.41
NL (%)	7.18	24.9	15.5	3.605	34.67	17.31	12.48	27.062	20.23
DRL (ohm.m)	0.77	8.82	3.26	0.599	22.94	3.36	0.285	4.934	0.76
DL (gm/cc)	2.27	2.74	2.49	2.184	2.843	2.52	2.219	2.698	2.37

Fortunately, the optimum structure for all the seven developed *ANNs* is one hidden layer with 12 neurons, as shown in Figure (6).

Open Access
No. 38, March 2023, pp. 56-73
P- ISSN: 2220-5381
E- ISSN: 2710-1096

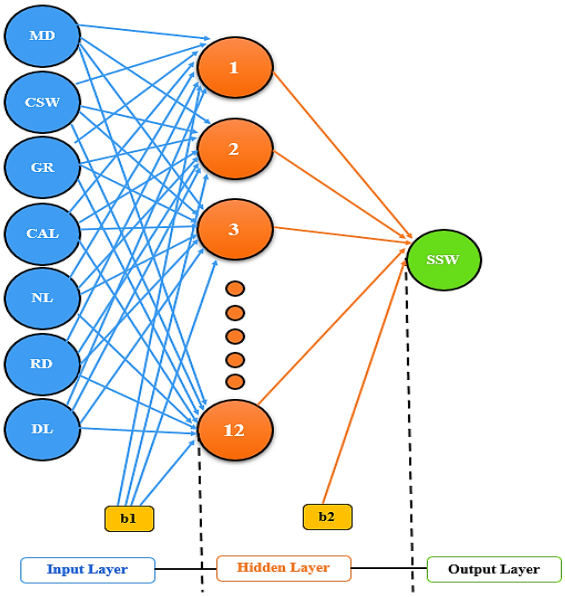

Fig. (6): Structure of all constructed *ANNs*.

3. Results and Discussion

The results of the developed *ANNs* are analyzed based on statistical values of average percent error (*APE*), absolute average percent error (*AAPP*), standard deviation (*SD*), mean square error (*MSE*), and correlation coefficient R-Square (R^2) as demonstrated in the following equations:

$$APE = \frac{1}{n}\sum_{i=1}^{n}\left(\frac{Tmi-Tpi}{Tmi}\right) \quad (10)$$

$$AAPE = \frac{1}{n}\sum_{i=1}^{n}|Tmi - Tpi| \quad (11)$$

$$SD = \left(\frac{\sum_{i=1}^{n}(T_{p,i}-Tp_{avg})^2}{n}\right)^{0.5} \quad (12)$$

$$MSE = \frac{1}{n}\sum_{i=1}^{n}(T_{m,i} - T_{P,i})^2 \quad (13)$$

$$R^2 = 1 - \frac{\sum_{i=1}^{n}(T_{m,i}-T_{Pi})^2}{\sum_{i=1}^{n}(T_{m,i}-Tpavg)^2} \quad (14)$$

Where T_{mi}, T_{pi} and T_{pavg} are measured, predicted and averaged predicted *SSW*.

Table (6) shows that the results of *ANN* for each zone have insignificant differences from the results of *ANN* for all zones, with R^2 values increasing in a small percent while *APE*, *AAPE*, *MSE*, and *SD* decreasing in particular values. Zone C deviated from this behavior as

Open Access
No. 38, March 2023, pp. 56-73
P- ISSN: 2220-5381
E- ISSN: 2710-1096

expected due to existing of 100% water saturation and a high percentage of shale. Despite the fact that *DRL* existed at the input layer of *SSW* prediction *ANNs*, it represented an indicator for fluid type rather than water saturation, where existing high-water saturation in porosity reduces *SSW* by a large percentage. Existing high shale content in the C zone raises *SSW* where it is represented on *ANN* by *GR* and *CAL*.

Table (6) Summary of Statistical parameters of both *ANNs* parts.

Zone	APE	AAPE	MSE	SD	R^2
All Zones	-0.078	2.06	3.3	2.81	0.98
Zone A	-0.007	1.07	1.9	1.36	0.99
Zone B1	0.022	1.40	2.3	1.50	0.99
Zone B2	-0.025	1.10	1.2	1.20	0.99
Zone B3	0.019	0.98	1.63	1.12	0.99
Zone B4	-0.021	0.99	1.45	1.18	0.99
Zone C	0.045	1.80	2.8	2.51	0.96

Figures (7) and (8) have measured *SSW* against predicted *SSW* by *ANNs* on Y-axis with *MD* on X-axis. Figure (7) is containing *SSW* estimated form *ANN* of all zones while Figure (8) is including *SSW* from *ANNs* for each zone. As shown above, small enhancing percent of *SSW* estimated values from *ANNs* of each zone than results of all zones, except C zone due to explained reasons. Results demonstrated that differences in reservoir lithology and its fluid content are already considered by employing seven input parameters, so no need to make *ANN* for each zone and *ANN* model of all zones is recommended for *SSW* prediction for vertical wells penetrating different lithologies.

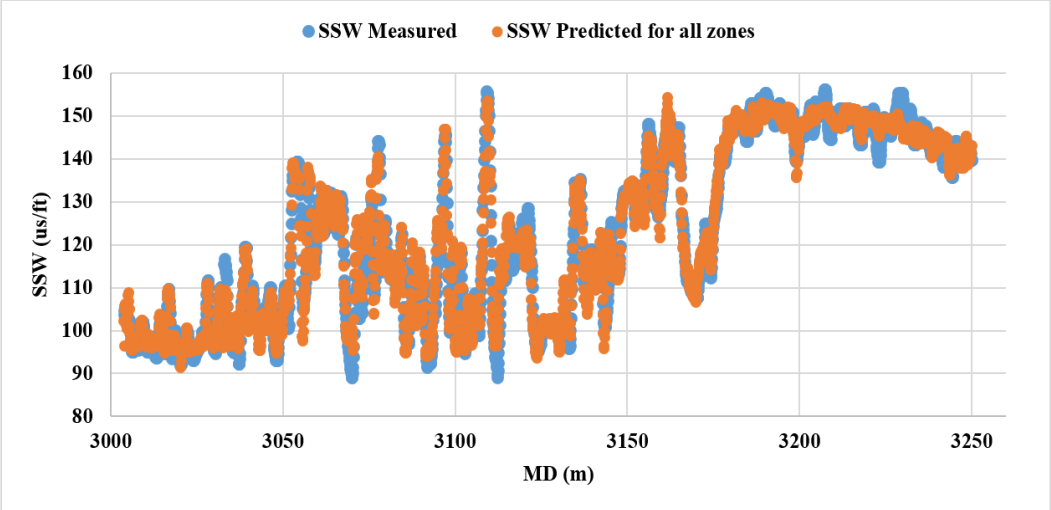

Fig. (7): Measured and Predicted *SSW* by *ANN* for all zones with *MD*.

Open Access
No. 38, March 2023, pp. 56-73
P- ISSN: 2220-5381
E- ISSN: 2710-1096

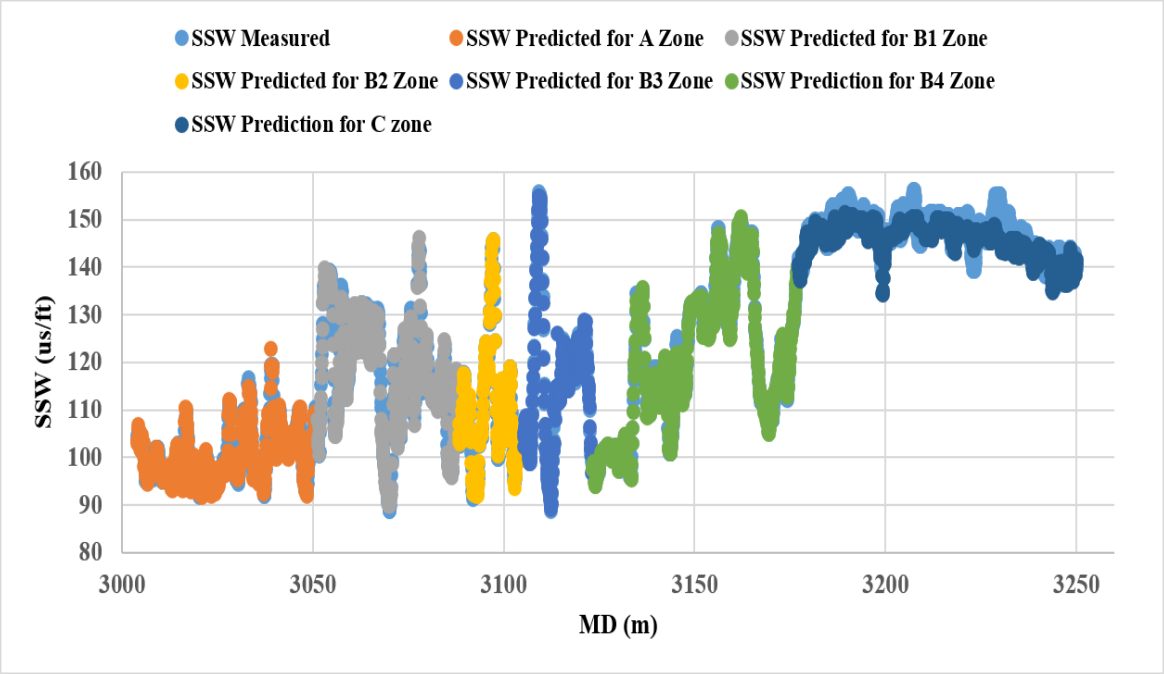

Fig. (8): Measured and Predicted *SSW* by *ANN* for each zone with *MD*.

The following mathematical model was obtained for representing the suggested *ANN* to simplify *SSW* calculation:

$$SSW = \sum_{j=1}^{12} W2_j \left(\frac{2}{1+e^{-2\left(W1_{j,1}\, MD + W1_{j,2}\, CSW + W1_{j,3}\, GR + W1_{j,4}\, CAL + W1_{j,5}\, NL + W1_{j,6}\, DRL + W1_{j,7}\, DL + b1_j\right)}} - 1 \right) + b2 \quad (15)$$

4. Conclusions

Reservoir heterogeneity is very influential on log tool measurements as well as *SSW*. At present, *ANN* is utilized to investigate the effect of reservoir heterogeneity on *SSW* prediction. The Iraqi vertical X well penetrated the Asmari reservoir with 2462 measured log points selected for this study. Based on formation assessment and available good data, the Asmari reservoir was classified into six zones (with different lithology and different fluid content): A, B1, B2, B3, B4, and C. Two runs of *ANN* were performed in this study to investigate the effect of lithology on *SSW*. Initially the team created a single *ANN* for all 2462 measured points, but in the second, we created six *ANNs*, one for each zone. *SSW* was an output of *ANNs* while *GR*, *CAL*, *CSW*, *NL*, *DL*, *MD*, and *DRL* were input parameters for the *ANNs* input layer. The dataset is classified into 30%, 15%, and 15% for training, testing, and validation respectively. Results demonstrated that two study ways of *ANNs* for all or for each zone had insignificant difference.

Open Access
No. 38, March 2023, pp. 56-73
P- ISSN: 2220-5381
E- ISSN: 2710-1096

Reservoir heterogeneity is already considered by utilized seven log parameters, so there is no need to classify reservoirs into multi-zones when predicting *SSW*. *ANN* model for all zones is recommended to calculate *SSW*. A mathematical model for all zones *ANN* was obtained to simplify *SSW* calculation for vertical wells penetrated reservoirs with different lithologies.

Nomenclatures

AAPE = Absolute average percent error

AI = Artificial Intelligent

ANN = Artificial neural network

APE = Average percent error

$b1_j$ = Input - hidden layers biases

CAL = Caliper log (in)

CSV = Compressional sonic velocity (ft/us) or (km/sec)

CSW = Compressional sonic wave time (us/ft)

DL = Density log (gm/cc)

DRL = Deep resistivity log (ohm.m)

GR = Gamma ray log (GAPI)

j = Hidden layer neurons

MD = Measured depth (length unit)

MSE = Mean square error

n = Neurons number of input layer

NL = Neutron log (%)

R^2 = Correlation coefficient

SD = Standard deviation

S_j = Summation of input weights and biases

SSV = Shear sonic velocity (ft/us) or (km/sec)

SSW = Sonic shear wave time (us/ft)

$W1_{ji}$ = Input – hidden layer neurons connection weights

$W2_j$ = Output - hidden layer connection weights

X_i = Input vector

T_{mi} = Measured shear sonic wave time (us/ft)

T_p = Predicted sonic shear wave time (us/ft)

T_{pavg} = Average predicted sonic shear wave time (us/ft)

Open Access
No. 38, March 2023, pp. 56-73
P- ISSN: 2220-5381
E- ISSN: 2710-1096

References

[1] S. Mohaghegh. "Virtual-Intelligence Applications in Petroleum Engineering: Part 1—Artificial Neural Networks," Society of Petroleum Engineers, SPE 58046, 2000.

[2] H. Li and J. F. Reynold, "On Definition and Quantification of Heterogeneity," Olkos, vol. 73, No. 2, pp. 280-284 (5 pages), 1995. https://doi.org/10.2307/3545921.

[3] W. Zhengquan, W. Qingcheng, Z. Yandong, and H. Li, "Quantification of spatial heterogeneity in old growth forests of Korean pine," Journal of Forestry Research, vol. 8, p. 65–73, 1997. https://doi.org/10.1007/BF02864969.

[4] P. J. R. Fitch, M. A. Lovell, S. J. Davies, T. Pritchard and P. K. Harvey, "An integrated and quantitative approach to petrophysical heterogeneity," Marine and Petroleum Geology, vol. 63, p. 82-96, 2015. https://doi.org/10.1016/j.marpetgeo.2015.02.014.

[5] T. Ertekin, J.H. Abou-Kassem, G.R. King, "Basic Applied Reservoir Simulation," Henry L. Doherty Memorial Fund of AIME, Society of Petroleum Engineers, Richardson, Texas, 2001.

[6] Schlumberger team, "heterogeneity, " Energy glossary website, 2022. https://glossary.slb.com/en/terms/h/heterogeneity.

[7] J. Schon, Basic Well Logging and Formation Evaluating, 1st edition, eBook at Bookboon, 2015.

[8] R.H. Allawi and M. S. Al-Jawad, " An Empirical Correlations to Predict Shear Wave Velocity at Southern Iraq Oilfield," Journal of Petroleum Research and Studies, no. 34 part 1, pp. 1-14, 2022. http://doi.org/10.52716/jprs.v12i1.586.

[9] W. M. Al-Kattan, " Prediction of Shear Wave velocity for carbonate rocks," Iraqi Journal of Chemical and Petroleum Engineering, vol.16, no.4, p. 45- 49, 2015.

[10] F.A. Hadi and R. Nygaard, " Shear Wave Prediction in Carbonate Reservoirs: Can Artificial Neural Network Outperform Regression Analysis," ARMA 18–905. 2018.

[11] M.R. Rezaee, A. K. Ilkhchi and A. Barabadi, " Prediction of shear wave velocity from petrophysical data utilizing intelligent systems: An example from a sandstone reservoir of Carnarvon Basin, Australia," Journal of Petroleum Science and Engineering, vol. 55, p. 201–212, 2007. https://doi.org/10.1016/j.petrol.2006.08.008.

[12] G.R. Pickett, "Acoustic Character Logs and Their Applications in Formation Evaluation," J Pet Technol, SPE-452-PA, vol. 15 (06), p.659–667 1963.

Open Access
No. 38, March 2023, pp. 56-73
P- ISSN: 2220-5381
E- ISSN: 2710-1096

[13] R.D. Carroll, "The determination of the acoustic parameters of volcanic rocks from compressional velocity measurements," Int. J. Rock Mech. Iin. Sci. vol. 6, pp. 557-579, 1969.

[14] J. P. Castagna, M. L. Batzle and R. L. Eastwood, "Relationships between compressional-wave and shear-wave velocities in clastic silicate rocks," Geophysics, vol. 50, no.4, 1985.

[15] M. L. Greenberg and J. P. Castagna, "Shear wave velocity estimation in porous rocks: Theoretical formulation, preliminary verification and applications," Geophysical Prospecting, vol. 40, p. 195-209, 1992.

[16] D. Freund, "Ultrasonic compressional and shear velocities in dry clastic rocks as a function of porosity, clay content, and confining pressure," Geophys. J. Inr. Vol. 108, pp. 125-135. 1992.

[17] T. M. Brocher, " Empirical Relations between Elastic Wave speeds and Density in the Earth's Crust," Bulletin of the Seismological Society of America, vol. 95, no. 6, pp. 2081–2092, 2005. 10.1785/0120050077.

[18] M. S. Ameen, B. G. D. Smart, J. M. Somerville, S. Hammilton and N. A. Naji, " Predicting rock mechanical properties of carbonates from wireline logs (A case study: Arab-D reservoir, Ghawar field, Saudi Arabia)," Marine and Petroleum Geology, vol. 26, p. 430–444, 2009.

[19] J. M. Al Said Naji, G. H. Abdul-Majeed, and A. K. Alhuraishawy, " Comparison of Estimation Sonic Shear Wave Time Using Empirical Correlations and Artificial Neural Network," paper accepted by Iraqi Journal of Chemical and Petroleum Engineering, 2022.

[20] M. A. Kassab and A. Weller, " Study on P-wave and S-wave velocity in dry and wet sandstones of Tushka region, Egypt," Egyptian Journal of Petroleum, vol. 24, p. 1-11, 2015.

[21] K. Tabari, O. Tabari and M. Tabari, "A Fast Method for Estimating Shear Wave Velocity by Using Neural Network," Australian Journal of Basic and Applied Sciences, vol. 5, no. 11, p. 1429-1434. 2011.

[22] A. Al Ghaithi and M. Prasad, "Machine learning with Artificial Neural Networks for shear log predictions in the Volve field Norwegian North Sea," SEG, International Exposition and 90th Annual Meeting, 2020.

Open Access
No. 38, March 2023, pp. 56-73
P- ISSN: 2220-5381
E- ISSN: 2710-1096

[23] H. H. Alkinani, A. T. Al-Hameedi, S. Dunn-Norman, R. E. Flori anf M. A. Al-Alwani, "Intelligent Data-Driven Analytics to Predict Shear Wave Velocity in Carbonate Formations: Comparison Between Recurrent and Conventional Neural Networks," Paper presented at the 53rd US Rock Mechanics/Geomechanics Symposium held in New York, NY, USA, 2019.

[24] J. M. Al Said Naji, G. H. Abdul-Majeed, and A. K. Alhuraishawy, " Prediction sonic shear wave by artificial neural network," paper submitted to Iraqi geological journal, 2022.

[25] W. I. Taher, M. S. Al Jawad and C. W. V. Kirk, "Reservoir study for Asmari reservoir/Fauqi field," Master thesis, University of Baghdad, Collage of Engineering, Iraq, 2011.

[26] Q. A. Abdul-Aziz and H. A. Abdul-Hussain, "Integration of Geomechanical and Petrophysical properties for estimating rate of penetration in Fauqi oil field Southern Iraqi," Doctorate dissertation, University of Baghdad, Collage of Engineerin, Iraq, 2021.

[27] J. E. Fox and T. S. Ahlbrandt, "Petroleum Geology and Total Petroleum Systems of the Widyan Basin and Interior Platform of Saudi Arabia and Iraq. U.S," Geological Survey Bulletin, 2002.

[28] L. Wang, " Study on Reservoir Heterogeneity in Block S," IOP Conf. Series: Earth and Environmental Science, vol. 770, 2021.

[29] F. S. Kadhim, A. Samsuri and Y. Al-Dunainawi, " ANN-Based Prediction of Cementation Factor in Carbonate Reservoir," SAI Intelligent Systems Conference, London, UK, pp 681-68. 2015.

[30] M.C. Popescu, V.E. Balas, L.P. Popescu, "Multilayer perceptron and neural networks," WSEAS Transactions on Circuits and Systems, Vol.8, pp. 579-588, 2009.

[31] G. H. Abdul-Majeed, F.S. Kadhim, F. H. Almahdawi, Y. Al-Dunainawi, A. Arabi and W. K. Al-Azzawi, "Application of artificial neural network to predict slug liquid holdup," International Journal of Multiphase Flow, Vol. 150, 2022. https://doi.org/10.1016/j.ijmultiphaseflow.2022.104004.

[32] E. Jorjani, C. S. Chehreh and S. H. Mesroghli, "Application of artificial neural networks to predict chemical desulfurization of Tabas coal," Fuel,Vol. 87, pp. 2727–3273. 2008.

[33] M. A. Razavi, A. Mortazavi and M.Mousavi, "Dynamic modeling of milk ultrafiltration by artificial neural network," J. Membrane , Vol. 120, pp. 47-58, 2003.

Open Access
No. 38, March 2023, pp. 56-73
P- ISSN: 2220-5381
E- ISSN: 2710-1096

https://doi.org/10.1016/S0376-7388(03)00211-4.

[34] M. Asoodeh and P. Bagheripour, "Prediction of Compressional, Shear, and Stoneley Wave Velocities from Conventional Well Log Data Using a Committee Machine with Intelligent Systems," Rock Mechanics and Rock Engineering, Vol. 45, pp. 45-63, 2012. doi 10.1007/s00603-011-0181-2.

[35] S. Maleki, A. Moradzadeh,R. G. Riabi, R. Gholami and F. Sadeghzadeh, "Prediction of shear wave velocity using empirical correlations and artificial intelligence methods," NRIAG Journal of Astronomy and Geophysics, Vol. 3, , pp. 70-81. 2014. https://doi.org/10.1016/j.nrjag.2014.05.001.

[36] H. Akhundi, M. Ghafoori and G. R. Lashkaripour, "Prediction of Shear Wave Velocity Using Artificial Neural Network Technique, Multiple Regression and Petrophysical Data: A Case Study in Asmari Reservoir (SW Iran)," Open Journal of Geology, Vol. 4, pp. 303-313, 2014.

[37] R. K. Abdul Majeed and A. A. Alhaleem, "Estimation of shear wave velocity from wireline logs data for Amara oilfield, Mishrif formation," Vol. 53, No.1A, Iraqi Geological Journal, 2020. https://doi.org/10.46717/igj.53.1a.R3.2020.01.30.